Styrene-Ethylene/Butylene-Styrene Blends for Improved Constrained-Layer Damping

JONAS ÖBORN, HANS BERTILSSON, MIKAEL RIGDAHL

Department of Polymeric Materials, Chalmers University of Technology, SE-412 96 Göteborg, Sweden

Received 19 January 2000; accepted 20 July 2000

ABSTRACT: The influence on the adhesion to some metal surfaces and the damping properties of various modified styrene-ethylene/butylene-styrene (SEBS) materials was evaluated. Modification of the different phases of the SEBS with resins was shown to have a large effect on the damping properties of the polymers, which were evaluated by dynamic mechanical analysis (DMA). A small amount of maleic anhydride grafted onto the EB block was found to lead to a significant improvement in the adhesion of the polymer to some metal surfaces without affecting the damping properties of the polymers. The results of the DMA tests on the polymers were used to calculate the composite loss factor (CLF) for a steel laminate, which consisted of two steel plates with a polymeric layer in between, according to the theory proposed by Ross, Ungar, and Kerwin. The calculated results were compared with the measured CLFs determined in vibrating beam tests (VBTs). The agreement between the calculated and measured values was quite fair, provided that the DMA values used for the calculations were recalculated to the actual higher frequencies used in the VBTs, using the time–temperature superposition principle. © 2001 John Wiley & Sons, Inc. J Appl Polym Sci 80: 2865–2876, 2001

Key words: constrained-layer damping; styrene-ethylene/butylene-styrene blends; glass transition; metal-polymer-metal laminate

INTRODUCTION

There has been an increased interest in the use of polymers for sound and vibration damping in recent years.[1] This is because noise has become a serious form of pollution. Materials with high damping properties therefore find numerous applications, especially in the automotive, aircraft, and building industries. Polymers are useful vibration damping materials near their glass-transition temperature where coordinated chain molecular motion dissipates mechanical energy as heat. Homopolymers generally have narrow glass-transition regions (20–30°C); when temperature becomes a significant variable, the narrow temperature range of the glass transition causes most homopolymer damping materials to fail.[2]

The glass transition of a given homopolymer at a given frequency can be shifted in temperature within a certain range. One way is to use a plasticizer, which lowers the glass-transition temperature. Another way is to use an inorganic filler in the polymer. The total effect of the added filler can be both a broadening of the glass transition and a rise in the peak temperature.[1,3–5] A third general way of changing the glass-transition temperature is through copolymerization.[1] Polymer

Correspondence to: M. Rigdahl (rigdahl@polymm.chalmers.se).

Contract grant sponsors: Collins & Aikman Automotive Interior Systems Europe; Swedish Council for Vehicle Research.

Journal of Applied Polymer Science, Vol. 80, 2865–2876 (2001)
© 2001 John Wiley & Sons, Inc.

blends and multicomponent systems can also be used to control and widen the damping properties of polymers.[1,5–8] The properties of a polymer blend are to a large extent determined by its morphology. There are several studies on how to control this.[9–11]

The shear loss modulus (G'') and the loss factor (tan δ) are both measures of the sound and vibration damping, and they describe the transformation of mechanical energy into heat. The integral of the linear loss shear modulus over a temperature range is the loss area (LA), and the integral of the linear tan δ over a temperature range is the tan δ area (TA). From an engineering point of view, there are basically two kinds of damping modes of interest when using polymers. Large LA values are desired for extensional damping (putting a coating on a vibrating structure), and large TA values are desired for constrained-layer damping (putting a layer of damping polymer between two structures, sandwich type). Qualitatively, this means that extensional damping needs a material in the high modulus region of its glass-transition range, whereas constrained-layer damping needs a material in the low modulus region of its glass-transition range.[6] Whenever any type of constraining layer is applied on top of a damping layer, the constrained-layer damping is likely to exceed the extensional damping. This is because the shear deformation in the damping layer with constrained layers dissipates more energy than the bending deformation in an extensional damping layer. In fact, even in an equal-weight comparison, applied treatments that utilize shear damping are likely to be more effective than those employing extensional damping.[12,13]

Metal-polymer-metal sandwich composite materials are often used for vibration damping. In these three-layer composites the viscoelastic properties of the polymer inner layer and the interactions between the layers are both of major importance. The interactions at steel–polymer interfaces were studied in order to evaluate the influence on the adhesion[14–16] and the influence on the damping properties.[14] The influence of surface energy on the adhesive performance was studied using contact angle hysteresis.[17]

Such composites can be used in a wide range of applications, for example, in the automotive industry as different covers, oil pans, and panels or in washing machines, refrigerators, and so forth.[18–22] Important issues for the use of these steel laminates are their welding and forming properties. Consequently, studies were performed in order to optimize these parameters[18,23] and also to see how the acoustic properties of the polymer inner layer are affected by a paint bake cycle[24] or by resistance spot welding.[25] A common way of solving the welding problem is to add a conductive metal powder in the polymer inner layer.[18,20,21] It is often claimed that press formability of laminated steel is strongly influenced by the adhesive strength of the core resin[14,15,21] and that a higher adhesive strength gives better press formability.[18] Because the polymer inner layer is viscoelastic, it has to be acoustically optimized with regard to its operational temperature and frequency ranges. On the other hand, the processability has to be optimized at room temperature because this is the temperature at which the laminate is normally processed. This may cause some problems and finite element methods were used to simulate damping, forming, and bending of vibration-damping steel.[7,19,26–29]

It has been claimed that to have an efficient damping level the composite loss factor (CLF) of the steel laminate should exceed 0.05[30] or sometimes 0.10 using the vibrating beam test (VBT).[31] In this study we chose to use as the criteria for good damping the width of the temperature interval where the CLF of the laminate exceeds 0.10 and where the tan δ for the polymers exceeds 0.30.[30] This correlation between the two loss factor values was obtained using the Ross, Ungar, and Kerwin (RUK) theory.[32]

The aim of this work was to clarify which polymer systems that have good damping properties over a wide temperature range and that could thus be interesting to use as damping layers for constrained-layer damping.

EXPERIMENTAL

Materials

The materials used in this study were steel laminates consisting of two steel beams with a very thin polymeric layer in between them.

Metal

The metallic part of the sandwich used for the T-peel tests and the shear strength tests was 0.6 mm thick hot-zinced steel from SSAB Tunnplåt AB (Dogal F36 Z275 chromated). The T-peel tests were also carried out with 0.3 mm thick aluminum to avoid too much energy being used to bend

the metal while peeling the sandwich apart. The steel used for the VBTs was 1.0 mm thick cold-rolled steel of SS 1142-32 quality.

Polymers

The polymers used for the inner layer were linear triblock copolymers of styrene-ethylene/butylene-styrene (SEBS, Shell Chemical Company). We used four different SEBS materials in this study: Kraton G-1652, Kraton G-1657, Kraton FG-1901X, and Kraton FG-1924X. Kraton G-1652 (SEBS-30) is a classical triblock SEBS with a polystyrene content of 30 wt %, and Kraton G-1657 (SEBS-13) is a SEBS/SEB type with a polystyrene content of 13 wt % and a diblock (SEB) content of 30 wt %. The last two Kraton materials are maleic anhydride functionalized, which means that they have maleic anhydride bound to the EB phase. Kraton FG-1901X (SEBS-MA-30) has 1.7 wt % bound maleic anhydride and a polystyrene content of 30 wt % (similar to SEBS-30). Kraton FG-1924X (SEBS-MA-13) has 1.0 wt % bound maleic anhydride, a polystyrene content of 13 wt %, and a diblock (SEB) content of 30 wt % (similar to SEBS-13).

Modifier Resins

In order to change and control the softening point of the SEBS polymers, some modifying resins were added to the polymers in different amounts (10–75 wt %). The resins used were Regalite R1100 (R1100), Regalite R1090 (R1090), and Hercures AR100 (AR100) from Hercules. The Regalite resins are low molecular weight, fully hydrogenated, thermoplastic hydrocarbon resins. They are aliphatic and therefore compatible only with the elastomeric midblock of the SEBS, which is the EB block. The AR100 is a low molecular weight, modified aromatic hydrocarbon resin, which is compatible only with the polystyrene end blocks of the SEBS.

Stabilizers

During the oven drying before the lamination, the coated polymer formulations were exposed to air. Two stabilizers were added to protect the polymer formulations from oxygen attack during this processing stage: Irganox 1010 (Ciba–Geigy) and Perkacit ZBDC (Flexsys). The amount of each of the stabilizers added was 1 wt % of the SEBS content.[33] Irganox 1010 is of the tetrakis[methylene 3-(3′,5′-di-*tert*-butyl-4′-hydroxyphenyl)-propionate]methane type and Perkacit ZDBC is of the zinc dibutyldithiocarbamate type.

Sandwich Lamination

The sandwich samples were produced in laboratory curtain coating equipment. Both of the steel sheets of the laminate were coated with a solution in aromatic naphtha of the polymer formulation, dried in an oven at 150°C for 5 min, and then directly laminated together under pressure. The lamination was done in a laboratory rolling mill under a pressure of 0.2 MPa and at a speed of 3 m/min. The dry coating thicknesses were 25 μm on each sheet to give a total polymer layer of 50 μm in the laminate. The T-peel and shear strength samples were 250 $\times$ 150 mm, and the VBT samples were 250 $\times$ 15 mm. The steel beams for the VBTs were cleaned with methyl ethyl ketone before being coated. All the other samples had a clean delivery surface from the supplier and required no further cleaning.

Methods

Several different methods were used to characterize the properties of the polymer and the laminate.

Dynamic Mechanical Analysis (DMA)

These tests were carried out on the polymers as temperature sweeps at 1 Hz using a torsional rectangular geometry and a temperature ramp increase of 5°C/min. The free sample length was 15–18 mm, the width was approximately 10 mm, and the thickness was about 2 mm. The equipment used was a Rheometrics RDAII with Rhios version 4.3.2 software.

T-Peel Tests

The T-peel tests were performed according to ASTM D 1876-72 with some modifications regarding the sample size.[34] The sample width was 25 mm, the tested length was 200 mm, and the clamped T ends were 50 mm each. The speed of the clamps was 25 mm/min, and the tests were performed using a Zwick 1455 with a 20-kN load cell.

Shear Strength Test

The shear strength tests were carried out according to Volvo Corporation standard STD 1024,

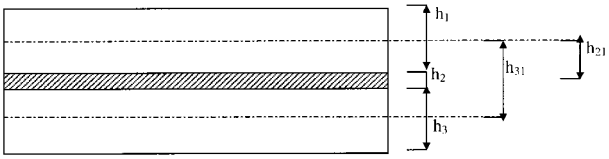

Figure 1 A schematic diagram of the laminate configuration.

2815 which is a type of overlap test.[35] The sample size was 25 × 150 mm with an overlap area of 25 × 25 mm in the middle of the sample. The speed of the clamps was 2.5 mm/min, and the tests were performed with Zwick 1455 with a 20-kN load cell.

VBT Runs

Acoustic evaluations of the laminates were done by measuring the CLF for the sandwiches at different temperatures and different frequencies using the vibrating beam method according to ASTM E 756-83.[31] For this type of test specimen, the dynamic response is obtained in terms of frequency, the half-power bandwidth (3 dB down points) of each mode in the response spectrum, the geometric properties of the bar, and the densities of the materials constituting the specimen. The sample width, tested free length, and thickness were 15.0, 200, and 2.05 mm, respectively. The software used was VBT Measurement version 1.0 (Beta 7) from Damping Technology Inc.[36]

Calculations

To calculate and predict the damping properties of the laminate from the properties of its constituent layers, the following two methods were used.

Calculated CLF (CCLF)

The RUK method calculates the damping effectiveness of a laminate consisting of two elastic plates with an intermediate viscoelastic layer.[32] This method gives the system loss factor η of a constrained sandwich beam (Fig. 1) by the expression

$$\eta = \frac{(\tan\delta)gY}{1 + (2 + Y)g + (1 + Y)[1 + (\tan\delta)^2]g^2} \quad (1)$$

where Y is the stiffness parameter of the laminate, g is the shear parameter, and $\tan\delta$ is the loss factor of the viscoelastic layer. The g is defined as

$$g = \frac{G'}{\rho^2 h_2}\left(\frac{1}{E_1 h_1} + \frac{1}{E_3 h_3}\right) \quad (2)$$

where E_1 and E_3 are the elastic moduli of the top and bottom layers, respectively; G' is the shear storage modulus of the viscoelastic polymer layer; h_1, h_2, and h_3 are the thicknesses of the corresponding layers; and ρ is the wave number of the laminate at the resonance frequency. The $\tan\delta$ and G' are both functions of temperature. The wave number is related to the resonance frequency by

$$\rho = \sqrt[4]{\omega^2 \frac{m}{B}} \quad (3)$$

where $\omega = 2\pi/f_n$, f_n is the resonance frequency of the nth mode, B is the flexural rigidity, and m is the mass per unit area of the laminate. The expression of Y is given by

$$\frac{1}{Y} = \left(\frac{E_1 h_1^3 + E_3 h_3^3}{12 h_{31}^2}\right)\left(\frac{1}{E_1 h_1} + \frac{1}{E_3 h_3}\right) \quad (4)$$

where h_{31} is the distance between the neutral planes of the two elastic layers.

For a symmetric laminate with constant thickness of each layer, as in the present case, the Y is a constant and the g is proportional to (G'/ρ^2). In addition, it can be seen in eq. (1) that, for constant $\tan\delta$ and constant Y, there is an optimal shear parameter g_{opt} where η attains a maximum. Furthermore, η increases with decreasing g value when g is larger than g_{opt} and decreases when g is smaller than g_{opt}. For a given polymeric inner layer, it can be seen in eq. (3) that the wave number is, to a good approximation, a function of the resonance frequency only and can be expressed as $\rho = \rho(f_n)$. In this case, the shear parameter is of the form

$$g = \frac{AG'}{\rho^2(f_n)} \quad (5)$$

where A is a constant depending on the laminate configuration and on the elastic modulus of the steel sheets. Thus, η can be calculated via eq. (1) using selected values of f_n, G', and $\tan\delta$.

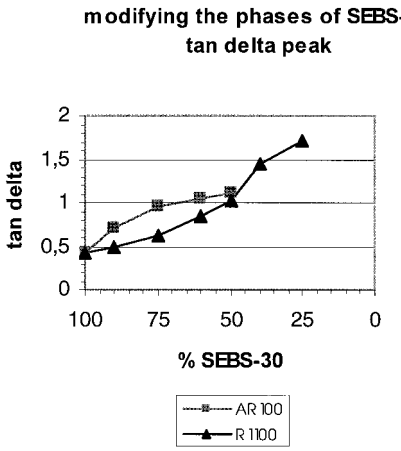

Figure 2 The height of the damping peaks for the different phases of SEBS-30 versus the amount of SEBS-30 in the SEBS-30/R1100 (EB phase) and SEBS-30/AR100 (styrene phase) systems.

$$\eta = \eta(f_n, G', \tan \delta) \quad (6)$$

The calculations were carried out using the material properties of the polymer obtained from the DMA tests described earlier. The thicknesses of the three layers in the calculations were the same as in the VBTs. It should be noted that the RUK model does not take into account any influences of the adhesion between the viscoelastic layer and the plates (i.e., perfect adhesion is assumed).

Time–Temperature Superposition

The available DMA instrument was limited to a frequency range up to 16 Hz whereas the frequencies of interest for the CLF were between 200 and 1500 Hz. To obtain appropriate results when using the model to calculate the CLF at these high frequencies, the shear modulus and loss factor of the polymer layer in this frequency range are required. The time–temperature superposition principle[37] in the form of the William–Landel–Ferry (WLF) equation was therefore used to obtain master curves for the viscoelastic properties of the polymer over a wide frequency range. The WLF equation may not be ideally suitable for modified polymers, but it was used to obtain estimates for comparison with the measured VBT results.

Temperature sweep measurements over the glass-transition region for several different frequencies (0.03–10 Hz) were carried out on the DMA equipment. From these results the constants in the WLF equation were obtained as $C_1 \approx 9$ and $C_2 \approx 40$°C for the unmodified polymer and in the same range for the modified systems. Using these values, the viscoelastic properties at the higher frequencies could be calculated and used in the RUK model.

RESULTS AND DISCUSSION

DMA Testing

Modification of the different phases of the SEBS with resins had a large influence on the damping properties. When R1100 was added, the tan δ peak of the EB phase increased in magnitude with increasing amounts of the resin and also became wider, as shown in Figures 2 and 3 and Table I. The temperature corresponding to the tan δ peak of the EB phase was also shifted to higher values with increasing amounts of R1100, because the softening point of R1100 is significantly higher than the softening point of the EB phase, which is shown in Figure 4. On the other hand, the tan δ peak for the styrene phase decreased in magnitude with increasing amounts of R1100 and no peak was found when the R1100 content was higher than 40 wt %. This was because the styrene peak was hidden in the decreased melt viscosity of the blend when R1100 was added and therefore could not be measured. A comparison of SEBS-30 with SEBS-MA-30 showed that a small amount of maleic anhydride grafted onto the EB block did not affect the damping properties.

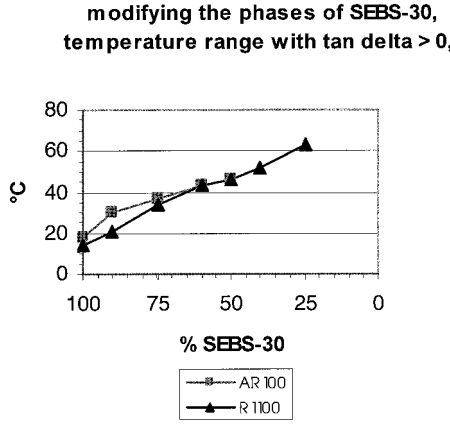

Figure 3 The width of the damping peaks for the different phases of SEBS-30 versus the amount of SEBS-30 in the SEBS-30/R1100 (EB phase) and SEBS-30/AR100 (styrene phase) systems.

Table I Max tan δ and Temperature of Max tan δ for EB Phase and Different Modifying Resins

Composition	Ratio	Max tan δ	*T* (Max tan δ) (°C)
SEBS-30/R1100	100/0	0.41/0.42	−46/95
	75/25	0.62/0.31	−30/85
	50/50	1.03/—	3.5/—
SEBS-MA-30/R1100	100/0	0.41/0.42	−45/100
	75/25	0.59/0.38	−24/92
	50/50	1.07/—	3.5/—
SEBS-30/R1090	100/0	0.41/0.42	−46/95
	75/25	0.69/0.36	−27/89
	50/50	1.07/—	2.5/—
SEBS-13/R1100	100/0	1.00/—	−49/—
	50/50	1.23/—	−6.5/—
SEBS-MA-13/R1100	100/0	0.75/—	−49/—
	50/50	1.32/—	−5.5/—

The influence of the styrene content in the SEBS on the damping behavior was evaluated by comparing SEBS-30 with SEBS-13 and by comparing SEBS-MA-30 with SEBS-MA-13 when the EB phase was modified (Table I). For the pure SEBS samples with 13 wt % styrene, only the tan δ peak for the EB phase could be found, as mentioned above, when more then 40 wt % R1100 was added. The damping peak for the EB phase was higher for the samples with higher EB content as we expected, and it was located at a temperature 3–4°C lower than that of the samples with lower EB content (SEBS-30 and SEBS-MA-30). When R1100 was added to modify the EB phase, the tan

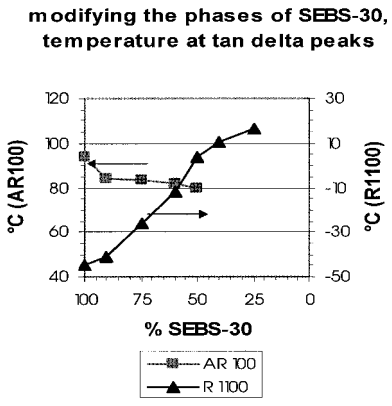

Figure 4 The location of the damping peaks along the temperature axis versus the amount of SEBS-30 in the SEBS-30/R1100 (EB phase) and SEBS-30/AR100 (styrene phase) systems.

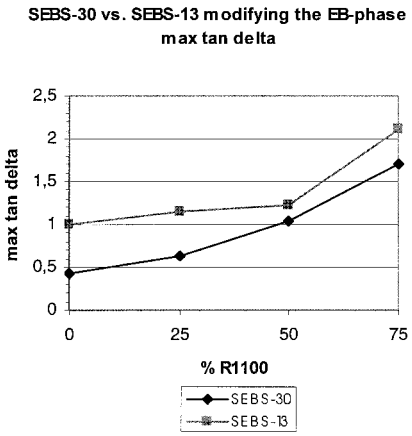

Figure 5 A comparison of the height of the damping peaks of SEBS-30/R1100 and SEBS-13/R1100.

δ of that phase increased with increasing amount of added resin (Fig. 5) and the peak became wider (Fig. 6). This figure also shows that the change was not as pronounced as for the samples of lower EB content and that the temperature at which the tan δ for the EB phase reached a maximum increased with an increasing amount of R1100.

The effect of the softening point of the added resin on the damping behavior was studied by comparing the effect of R1100, which has a softening point at 100°C, with that of R1090, which has a softening point at 90°C, using the ring and ball method. The observed difference in damping behavior was quite small, but the samples modified with R1090 showed a tendency to have damp-

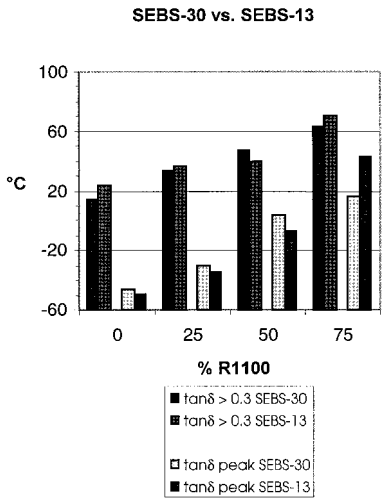

Figure 6 A comparison of the width and the location along the temperature axis of the damping peaks of SEBS-30/R1100 and SEBS-13/R1100.

Table II Max tan δ, Temperature of Max tan δ, and Width of tan δ for Styrene Phase

Composition	Ratio	Max tan δ	T (Max tan δ) (°C)	ΔT (tan δ > 0.3) (°C)
SEBS-30/AR100	100/0	0.41/0.42	−46/95	13/17
	50/50	0.17/1.18	−45/80	—/57
SEBS-MA-30/AR100	100/0	0.41/0.42	−45/100	15/19
	50/50	—/1.05	—/77	—/68.5
SEBS-13/AR100	100/0	1.00/—	−49/—	24/—
	50/50	—/1.16	—/74	—/56
SEBS-MA-13/AR100	100/0	0.75/—	−49/—	24.5/—
	50/50	—/1.05	—/72	—/65

ing peaks for the EB phase that were a few degrees lower than those of the corresponding samples modified with R1100. This was as expected.

When AR100 was added to modify the styrene phase, the tan δ peak of the styrene phase increased with an increasing amount of resin and it became wider (Figs. 2, 3, Table II). The temperature at which the tan δ peak for the styrene phase was located decreased somewhat with increasing amounts of AR100 (Fig. 4) whereas the height of the tan δ peak for the EB phase decreased. The styrene peak was not shifted along the temperature axis as it was when the EB phase was modified with R1100, because the softening point of AR100 was approximately the same as that of the styrene phase (100°C). A comparison of the SEBS-30 with SEBS-MA-30 showed that a small amount of maleic anhydride grafted onto the EB block did not affect the damping properties when the styrene phase was modified.

The effect on the tan δ peak value and on its location of the styrene content in the SEBS was also evaluated by comparing SEBS-30 with SEBS-13 and by comparing SEBS-MA-30 with SEBS-MA-13 when the styrene phase was modified. In these cases, no significant differences between the samples were noted with regard to either the height and the width of the damping peak or its temperature location (Table II).

Table III T-Peel Test on 0.3-mm Aluminum

Composition	Ratio	T-Peel Strength (N/mm)
SEBS-30/R1100	100/0	0.32
	75/25	0.54
	50/50	2.01
SEBS-MA-30/R1100	100/0	2.60
	75/25	2.69
	50/50	3.06
SEBS-13/R1100	100/0	0.58
	50/50	1.23
SEBS-MA-13/R1100	100/0	2.08
	50/50	1.81

T-Peel Test

The maleic anhydride groups grafted onto the SEBS led, as expected, to a great improvement in the T-peel strength (see Tables III, IV). The force needed to peel the laminate apart was more than 8 times greater for the pure SEBS-MA-30 than for the pure SEBS-30 and up to 1.67 times greater for the SEBS-MA-30 containing 50 wt % R1100 compared to the SEBS-30 containing 50 wt % R1100. In all cases with the exception of SEBS-MA-13, the T-peel strength increased with increasing amounts of R1100. The T-peel tests using 0.6-mm steel were first carried out, but in the case of materials exhibiting a low adhesion between the polymer layer and the steel no useful results were obtained because the adhesion was too low in relation to the bending stiffness of the steel specimen. When studying the samples during the peel test, it could be clearly seen that the radius at the apparent point of delamination between the polymeric layer and the substrate became larger as

Table IV T-Peel Test on 0.6-mm Dogal Steel

Composition	Ratio	T-Peel Strength (N/mm)
SEBS-30/R1100	100/0	1.24
	75/25	1.43
	50/50	1.86
SEBS-MA-30/R1100	100/0	2.03
	75/25	2.86
	50/50	3.10

Table V Shear Strength Test on 0.6-mm Dogal Steel

Composition	Ratio	Shear Strength (MPa)
SEBS-30/R1100	100/0	0.64
	75/25	1.02
	50/50	4.41
SEBS-MA-30/R1100	100/0	4.74
	75/25	5.30
	50/50	6.55
SEBS-13/R1100	100/0	0.63
	50/50	2.66
SEBS-MA-13/R1100	100/0	5.39
	50/50	4.72

the adhesion values became lower. In order to avoid too much energy being spent in bending the metal instead of peeling the laminate apart, 0.3-mm aluminum foil was used in the laminates instead of 0.6-mm steel. As can be seen in Tables III and IV, there was almost no difference between the results obtained with the two metal substrates when the adhesion was high. For the samples with poor adhesion, the differences between the steel and aluminum samples were large and they could not be compared because most of the energy was spent on bending the steel specimen. The adhesion differences between the steel-supported samples could not be compared for the same reason. The main conclusion to be drawn from these results was that maleic anhydride apparently had a positive effect on the adhesion.

Shear Strength Test

As expected, the maleic anhydride groups grafted onto the SEBS also led to a great increase in the shear strength, as shown in Table V. The value for pure SEBS-MA-30 was more than 7 times greater than that for SEBS-30, and for the blend with 50 wt % R1100 the increase was more than 50%. In all cases except SEBS-MA-13, the shear strength increased with increasing amounts of R1100. This behavior was similar to that displayed by the T-peel strength.

VBT Runs

The VBTs were performed on steel laminates in order to compare the damping of the laminates with the damping of the polymers recorded by DMA. The effect of adding R1100 to modify the EB phase was qualitatively the same as that observed in the DMA measurements, which was expected; the damping peak of the EB phase increased in magnitude with increasing amounts of resin and also became wider (see Table VI). The temperature corresponding to the maximum of the damping peak for the EB phase was also shifted to higher values with increasing amounts of R1100. When the DMA and VBT results were compared in more detail, we observed that the damping peaks in the VBT measurements were shifted to higher temperatures, which was due to the fact that the VBT measurements were performed at much higher frequencies of 200–2000 Hz compared to 1 Hz with the DMA measurements.[30] The heights of the damping peaks were much lower for the stiffer steel-laminated VBT samples than for the DMA samples. The results of the VBT measurements for the second mode are given in Table VI, and an example is provided in Figure 7 for different vibration modes. The length of the VBT samples was chosen to locate the resonance frequency of the second mode at approximately 200 Hz at the maximum damping temperature (Fig. 8). With the equipment used the

Table VI Composite Loss Factor (CLF) for Mode 2

Composition	Ratio	Max CLF	T (Max CLF) (°C)	ΔT (CLF > 0.1) (°C)
SEBS-30/R1100	100/0	0.069/0.075	−30/95	—
	75/25	0.11/—	0/—	−5 − 5 = 10
	50/50	0.31/—	40/—	22 − 65 = 43
SEBS-MA-30/R1100	100/0	0.116/0.043	−30/90	−30 − −22 > 8
	75/25	0.15/—	0/—	−12 − 13 = 25
	50/50	0.29/—	40/—	23 − 66 = 43
SEBS-13/R1100	100/0	0.30/—	−30/—	−30 − −11 > 19
	50/50	~ 30/—	~ 30/—	6 − 49 = 43
SEBS-MA-13/R1100	100/0	0.25/—	−30/—	−30 − −18 > 12
	50/50	~ 0.32/—	~ 0.32/—	12 − 57 = 45

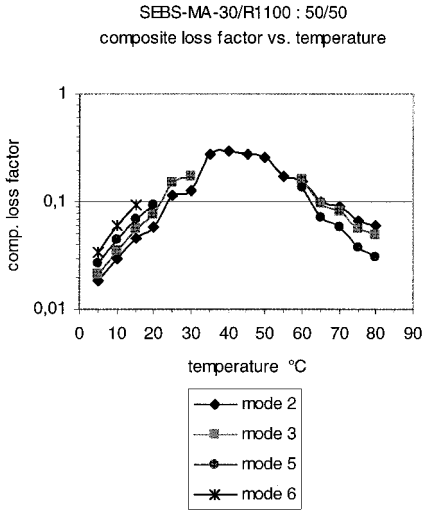

Figure 7 The composite loss factor versus the temperature for the 50/50 SEBS-MA-30/R1100 system. The results obtained for different vibration modes are shown.

measurements could not be performed at temperatures below −30°C; consequently, the damping peak of the EB phase in the pure SEBS could not be found.

The influence of the styrene content in the SEBS on the damping behavior was evaluated by comparing SEBS-30 with SEBS-13 and SEBS-MA-30 with SEBS-MA-13 when the EB phase was modified with R1100. The results were qualitatively comparable with the DMA results. For the pure SEBS-13 and SEBS-MA-13, the damping peak for the EB phase could not be found because it was located below −30°C. The samples with 13 wt % styrene content and modified with 50 wt % R1100 had their damping peaks at a temperature 8–10°C lower than that of the corresponding samples with 30 wt % styrene content.

The choice of using the temperature span where the tan δ of the polymer exceeded 0.3 as a criteria for obtaining a CLF exceeding 0.1 from the VBT measurements[30] worked well only for the samples exhibiting high damping and containing 50 wt % R1100. An explanation of this may be that the shear modulus of the polymers was too high at lower temperatures and too low at higher temperatures to produce sufficient shear damping in the laminates.

No really significant difference in the composite damping properties between the SEBS and the corresponding SEBS-maleic anhydride laminates could be seen. This means that there was no significant influence of the adhesion on the damping properties in this case. In earlier studies it was found that the loss factor increases with increasing peel energy until a threshold value beyond which the adhesion has no influence on the loss factor peak.[14] On the other hand, the samples with the poorest adhesion were also those that had the lowest damping properties.

CCLF and Time–Temperature Superposition

The CLFs were calculated using the theory proposed by Ross and colleagues[32] and the results from the DMA measurements, and they were compared with the CLFs determined by VBTs. The calculated results are shown in Table VII. When the CCLF values are compared with the DMA values used in the calculations, there is a shift upward in temperature for the calculated damping peak of the composite, which is attributable to the fact that the CCLF depends not only on the polymer loss factor but also on its shear modulus [cf. eq. (1)]. The decision to use the temperature span where the polymer loss factor exceeds 0.3 as a criterion for obtaining a CLF exceeding 0.1 did not work well for the same reason; the dependence of the CLF on the shear modulus has to be taken into account. When the RUK model is used, the shear modulus of the polymer has to be in the range of 2.3–4.7 MPa when the loss factor is greater than 0.3 in order to obtain a CCLF exceeding 0.1 at 200 Hz and in the range of 5.8–11.8 MPa at 500 Hz.

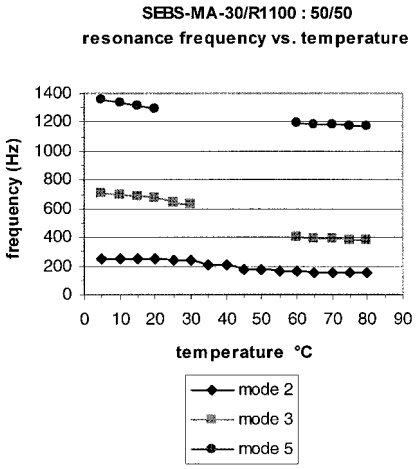

Figure 8 The resonance frequency for different vibration modes versus the temperature for the composite containing 50/50 SEBS-MA-30/R1100.

Table VII Calculated Composite Loss Factor (CCLF) at 200 Hz without WLF Correction

Composition	Ratio	Max CCLF	T (Max CCLF) (°C)	ΔT (CCLF > 0.1) (°C)
SEBS-30/R1100	100/0	0.025/0.139	−35/90	82 − 99 = 17
	75/25	0.098/0.083	−10/85	—
	50/50	0.218/—	10/—	1 − 24 = 23
SEBS-MA-30/R1100	100/0	0.023/0.128	−35/100	92 − 107 = 15
	75/25	0.074/0.107	−10/90	86 − 93 = 7
	50/50	0.250/—	10/—	−1 − 25 = 26
SEBS-13/R1100	100/0	0.160/—	−45/—	−49 − −36 = 13
	50/50	0.264/—	±0/—	−11 − 11 = 22
SEBS-MA-13/R1100	100/0	0.105/—	−40/—	−42 − −39 = 3
	50/50	0.293/—	±0/—	−11 − 14 = 25

There is also a difference in temperature location of the CLF peaks when the VBT results are compared with the calculations; the calculated peaks occur at significantly lower temperatures (Tables VI, VII). This difference is due to the fact that the RUK model used here does not account for the frequency dependence of the loss factor and the shear modulus of the polymer. The values used for the calculations are measured at 1 Hz and calculated for 200–1500 Hz. This can be corrected for to some extent by using time–temperature superposition[37] to evaluate the viscoelastic properties of the polymer at the higher frequencies to be used in the RUK model.[38] The corrected results for the CCLF are shown in Table VIII, and they may be compared with those in Tables VI and VII. Figures 9 and 10 show examples of the CCLF without and with the correction, respectively. They should be compared with the corresponding VBT measurements shown in Figure 7. As can be seen, the temperature location of the CCLF peaks fits the measured VBT results better after this correction, even though there still are some differences. The correction had no influence on the height of the CCLF or its width in temperature.

CONCLUSIONS

Modification of the different phases of SEBS with resins was found to have a large influence on the damping properties. The more resin added, the better were the damping properties of the SEBS. When the EB phase was modified, the temperature corresponding to the damping peak was shifted to higher temperatures with increasing amounts of resin added. This may be attributed to the substantially higher softening point of the R1100 resin than the EB phase. Because the AR100 resin used for modifying the styrene phase had approximately the same softening point as

Table VIII Calculated Composite Loss Factor (CCLF) at 200 Hz with WLF Correction

Composition	Ratio	Max CCLF	T (Max CCLF) (°C)	ΔT (CCLF > 0.1) (°C)
SEBS-30/R1100	100/0	0.025/0.139	−21/104	96 − 113 = 17
	75/25	0.098/0.083	8/103	—
	50/50	0.218/—	30/—	31 − 54 = 23
SEBS-MA-30/R1100	100/0	0.023/0.128	−21/114	106 − 121 = 15
	75/25	0.074/0.107	8/108	104 − 111 = 7
	50/50	0.250/—	30/—	29 − 55 = 26
SEBS-13/R1100	100/0	0.160/—	−25/—	−29 − −16 = 13
	50/50	0.264/—	25/—	14 − 36 = 22
SEBS-MA-13/R1100	100/0	0.105/—	−20/—	−22 − −19 = 3
	50/50	0.293/—	25/—	14 − 39 = 25

styrene, the shift in temperature of the corresponding peak was not as pronounced. A small amount of maleic anhydride groups grafted onto the EB phase in the SEBS did not effect the damping properties when the different phases were modified.

The maleic anhydride groups led to a great improvement of the adhesion of the polymer to a metal surface when peeling and shearing the laminate. However, there was no significant influence of the adhesion on the damping properties when the laminate damping (CLFs) of the corresponding SEBS and SEBS-maleic anhydride samples were compared.

The RUK method worked quite well for calculating the CLF of a laminate when the method was used together with time–temperature superposition of the viscoelastic properties of the polymer layer. The prediction of the location of the composite damping peak was quite reasonable and the model also qualitatively described the increase in the magnitude of the damping peak, as well as its broadening when resin was added to the polymer.

The analysis performed using the RUK model also indicated that it is not sufficient to evaluate the mechanical loss factor of the polymer used in order to assess the damping performance of the corresponding laminate. The shear modulus at the appropriate temperature and frequency is also important for the damping behavior of the laminate.

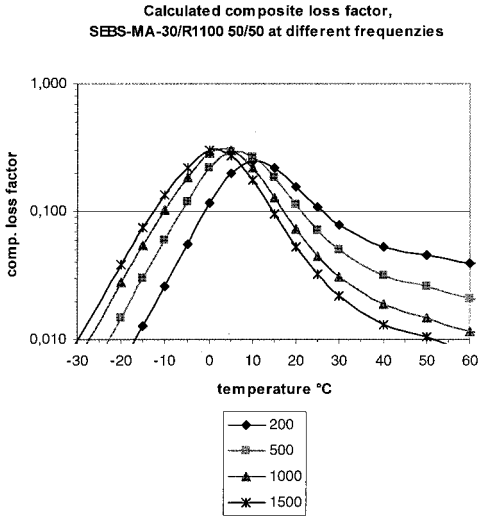

Figure 9 The calculated composite loss factor without WLF correction as a function of temperature at frequencies between 200 and 1500 Hz for 50/50 SEBS-MA-30/R110.

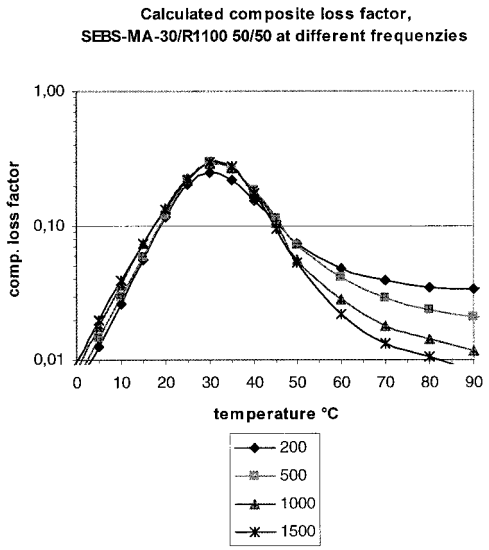

Figure 10 The calculated composite loss factor with WLF correction as a function of temperature at frequencies between 200 and 1500 Hz for 50/50 SEBS-MA-30/R110.

The authors wish to thank Dr. J. A. Bristow for the linguistic revision of the manuscript.

REFERENCES

1. Corsaro, R. D.; Sperling, L. H. Sound and Vibration Damping with Polymers, ACS Symposium Series 424; American Chemical Society: Washington, DC, 1990.
2. Weijiang, P.; Shucai, L. J Appl Polym Sci 1995, 58, 967.
3. Shucai, L.; Weijiang, P.; Xiuping, L. Int J Polym Mater 1995, 29, 37.
4. Wang, J.; Liu, R.; Li, W.; Li, Y.; Tang, X. Polym Int 1996, 39, 101.
5. Ting, R. Y.; Capps, R. N.; Klempner, D. Polym Mater Sci Eng 1989, 60, 654.
6. Hu, R.; Dimonie, V. L.; El-Aaser, M. S.; Pearson, R. A.; Hiltner, A.; Mylonakis, S. G.; Sperling, L. H. J Polym Sci B Polym Phys 1997, 35, 1501.
7. Andrén, P.; Falk, T. M Sc Eng Thesis, Applied Acoustics, Chalmers Univ. of Technology, Sweden, 1991.
8. Klempner, D.; Berkowski, L.; Frisch, K. C. Rubber World 1985, September, 16.
9. Hu, R.; Dimonie, V. L.; El-Aaser, M. S.; Pearson, R. A.; Hiltner, A.; Mylonakis, S. G.; Sperling, L. H. J Polym Sci A Polym Chem 1997, 35, 2193.
10. Tung, C.-J.; Hsu, T.-C. J. J Appl Polym Sci 1992, 46, 1759.
11. Liao, F.-S.; Su, A.-C.; Hsu, T.-C. J. Polymer 1994, 35, 2579.

12. Kerwin, E. M., Jr.; Ross, D. In Proceedings of the Third International Congress on Acoustics, L. Cremer (Ed.), Stuttgart, 1959; Elsevier, 1961, 1, 410–412.
13. Cremer, L.; Heckl, M.; Ungar, E. E. Structure-Borne Sound; Springer–Verlag: New York, 1973.
14. Cuillery, P.; Tatibouet, J.; Mantel, M. J Adhes Sci Technol 1998, 12, 271.
15. Bistac, S.; Vallat, M. F.; Schultz, J. J Adhes 1996, 56, 205.
16. Mantel, M.; Descaves, F. J Adhes Sci Technol 1992, 6, 357.
17. Bistac, S.; Kunemann, P.; Schultz, J. J Colloid Interface Sci 1998, 201, 247.
18. Nagai, H.; Shoita, T.; Taka, T.; Fukui, K. SAE Tech Pap Ser 1991, 911083.
19. Suh, Y. S.; Lee, J. Y. ASME PVP 1995, 321.
20. Sato, M.; Tanaka, Y.; Yutori, Y.; Nishikawa, H.; Miyahara, M. SAE Tech Pap Ser 1991, 910294.
21. Mathieu, S. Rev Métal-CIT 1994, October, 1481.
22. Suzukawa, Y.; Ikeda, K.; Morita, J.-I.; Katoh, A. SAE Tech Pap Ser 1992, 920249.
23. Oberle, H.; Commaret, C.; Magnaud, R.; Minier, C.; Pradere, G. Welding J 1998, 77, 8s.
24. Wang, P. C.; Fridrich, R. J. J Compos Mater 1996, 30, 1628.
25. Wang, P. C.; Fridrich, R. J. Welding J 1997, 76, 421s.
26. Cuillery, P.; Gaertner, R.; Tatibouet, J.; Mantel, M. J Appl Polym Sci 1997, 65, 2493.
27. von Finckenstein, E.; Kessler, L.; Steininger, V. Steel Res 1996, 67, 364.
28. Mignery, L. A. ASME DE 1995, 84-3.
29. Lu, Y. P.; Bai, J. M.; Sun, C. T. Key Eng Mater 1998, 141–143, 623.
30. Liao, F.-S.; Hsu, T.-C. J.; Su, A. C. J Appl Polym Sci 1993, 48, 1801.
31. ASTM E 756-83. Standard Method for Measuring Vibration-Damping Properties of Materials; American Society for Testing and Materials: Philadelphia, PA, 1989.
32. Ross, D.; Ungar, E. E.; Kerwin, E. M., Jr. Structural Damping; ASME: Atlantic City, NJ, 1959; p 49.
33. Erwins, E. E., Jr.; St. Clair, D. J.; Erickson, J. R.; Korcz, W. H. In Handbook of Pressure Sensitive Adhesive Technology, 2nd ed.; Satas, D., Ed.; Van Nostrand Reinhold: New York, 1989; p 317.
34. ASTM D 1876-72. Peel Resistance of Adhesives (T-Peel Test); American Society for Testing and Materials: Philadelphia, PA, 1983.
35. Andersson, T. Volvo Corporate Standard STD 1024, 2815, Issue 2. Adhesion between Sheet Metal and Layers of Insulation; Volvo Corporation, 1994.
36. Michael, C.; Lewis, T.; Jackson, P.; Nwankwo, O. SAE Tech Pap Ser 1999, 1, 181.
37. Ferry, J. D. Viscoelastic Properties of Polymers, 3rd ed.; Wiley: New York, 1980.
38. Liao, F.-S.; Hsu, T.-C. J. J Appl Polym Sci 1992, 45, 893.